

Supporting Material for

Connectivity Effects in Isomeric Naphthalenedinitrenes.

by

Paul R. Serwinski,^a Richard Walton,^a Jon A. Sanborn,^a Paul M. Lahti,^{*a} Tomonori Enyo,^b Daisuke Miura,^b Hideo Tomioka,^{*b} Athanassios Nicolaides^c

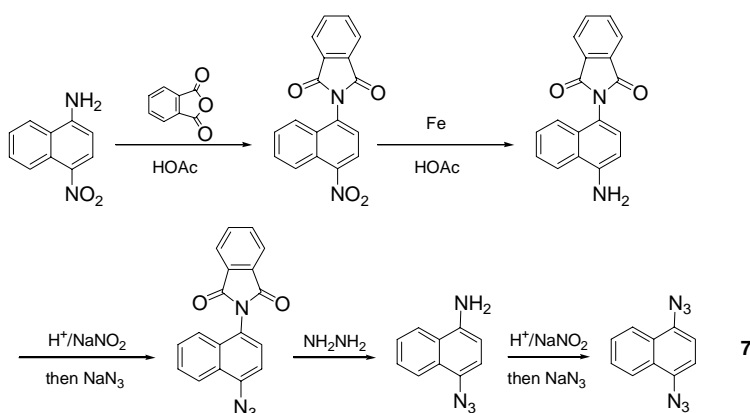
^aDepartment of Chemistry, University of Massachusetts, Amherst, MA 01003 USA

^bDepartment of Materials Science, Mie University, Tsu, Mie, 5148507 JAPAN

^cDepartment of Chemistry, University of Cyprus, Nicosia 1678, CYPRUS

Experimental Details.

Synthesis of 1,4-Diaزيدonaphthalene (7) was prepared according to a modified procedure of Hall and Patterson¹. A mixture of 1-amino-4-nitronaphthalene (3.0 g, 16 mmol), phthalic anhydride (3.1 g, 21 mmol) and acetic acid (200ml) was refluxed for 2 days. The reaction mixture was poured into ice-water, and precipitate was filtered, washed (acetic acid and water), and dried in vacuo to give 1-nitro-4-phthalimidonaphthalene (5.2 g, quantitative) as a yellowish solid: mp 233-235 °C; ¹H NMR (CDCl₃) δ 7.56 (d, *J* = 8.08 Hz, 1H), 7.61-7.86 (m, 3H), 7.87-7.91 (m, 2H), 8.01-8.06 (m, 2H), 8.30 (d, *J* = 8.08 Hz, 1H), 8.58 (dd, *J* = 8.64, 1.10 Hz, 1H).



To a stirred and refluxing solution of 1-nitro-4-phthalimidonaphthalene (5.0 g, 15.7 mmol) in acetone (200 ml), water (20 ml) and acetic acid (20 ml) was added powdered iron (3.4 g, 61 mmol) over a period of 1 hour. The reaction mixture was refluxed and stirred rapidly for an additional 7 hours. The excess iron and iron salt were filtered and washed with acetone. Acetone was evaporated from the filtrate, and the mixture was neutralized by aqueous sodium carbonate. Then deposited solid was filtered, washed with water, and dried in vacuo to give 1-amino-4-phthalimidonaphthalene (3.5 g, 77 %) as brown solid: mp 260-262 °C; ¹H NMR (CDCl₃) δ 4.38 (bs, 2H), 6.84 (d, *J* = 7.90 Hz, 1H), 7.47-7.52 (m, 3H), 7.82-7.87 (m, 4H), 7.98-8.00 (m, 2H).

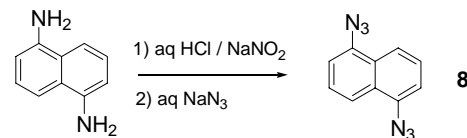
To a stirred and cooled solution of **1-amino-4-phthalimidonaphthalene** (2.0 g, 6.9 mmol), water (30 ml) and concentrated hydrochloric acid (30 ml) was added dropwise a solution of sodium nitrite (610 mg, 8.8 mmol) in water (15 ml) at 0-5 °C. To the stirred solution was added a solution of sodium azide (570 mg, 8.8 mmol) in water (15 ml) at 0-5 °C. After the reaction mixture was stirred for an additional hour, the resulting solution was extracted with CH₂Cl₂. Organic phase was washed (H₂O), dried (Na₂SO₄), filtered, evaporated, and dried in vacuo to give 1-azido-4-phthalimidonaphthalene (2.1 g, 97%) as a dark solid: ¹H NMR (CDCl₃) δ 7.37 (d, *J* = 7.90 Hz, 1H), 7.46 (d, *J* = 7.90 Hz, 1H), 7.54-7.56 (m, 3H), 7.84-7.87 (m, 2H), 8.00-8.03 (m, 2H), 8.20-8.23 (m, 1H); IR (KBr disk) ν 2119 (s), 1724 (s) cm⁻¹.

To a slurry of **1-azido-4-phthalimidonaphthalene** (2.1 g, 6.7 mmol) in methanol (30 ml) was added 100 % hydrazine hydrate (0.42 ml, 7.7 mmol) all at once and the mixture was stirred for an additional 30 min at room temperature. 3N sodium hydroxide was added to the mixture and the resulting solution was extracted with CH₂Cl₂. Organic phase was washed (H₂O), dried (Na₂SO₄), filtered, evaporated, and dried in vacuo to give 1-azido-4-aminonaphthalene (335 mg, 28 %) as a black solid: ¹H NMR (CDCl₃) δ 4.06 (bs, 2H), 6.73 (d, *J* = 8.08 Hz, 1H), 7.05 (d, *J* = 7.90 Hz, 1H), 7.45-7.50 (m, 2H), 7.72-7.77 (m, 1H), 8.04-8.08 (m, 1H).

To a stirred and cooled solution of **1-azido-4-aminonaphthalene** (335 mg, 1.8 mmol), water (15 ml) and concentrated hydrochloric acid (15 ml) was added dropwise a solution of sodium nitrite (170 mg, 2.2 mmol) in water (10 ml) at 0-5 °C. To the stirred solution was added a solution of sodium azide (160 mg, 2.2 mmol) in water (10 ml) at 0-5 °C. After the reaction mixture was stirred for an additional hour, the resulting solution was extracted with CH₂Cl₂. Organic phase was washed

(H₂O), dried (Na₂SO₄), filtered, evaporated, and dried in vacuo. The residue was purified by silica gel thin layer chromatography using *n*-hexane. The **1,4-naphthalenediazide** was eluted in the second fraction (130 mg, 34 %) as a white solid with mp 87-89 °C: ¹H NMR (CDCl₃) δ 7.23 (s, 2H), 7.54 (dd, *J* = 6.43, 3.31 Hz, 2H), 8.07 (dd, *J* = 6.43, 3.31 Hz, 2H); IR (Ar, 13 K) ν 2134 (s), 2118 (vs), 2101 (s), 1469 (m), 1401 (m), 1393 (m), 1299 (m), 1290 (m), 1164 (w), 1136 (w), 1026 (w), 811 (w), 766 (w), 659 (w), 632 (w) cm⁻¹; UV (Ar, 13 K) λ_{max} 225, 238, 312, 316, 326, 329, 341, 345 nm.

Synthesis of 1,5-Naphthalenediazide (8): To a suspension of 0.274 g (1.73 mmol) of freshly vacuum-sublimed 1,5-diaminonaphthalene (Aldrich) in 50 mL of 37 % HCl at 0 °C was added dropwise a solution of 0.292 g (4.24 mmol) of sodium nitrite in 10 mL of distilled water. After 1.5 h of stirring at 0 °C, a solution of 0.269 g (4.14 mmol) of sodium azide in 10 mL of distilled water was added dropwise to the yellow reaction mixture, which turned bright orange after 15 min of stirring. The reaction was worked up by treatment with 20 g of NaOH in 100 mL of distilled water (more NaOH pellets were added directly to the reaction to completely neutralize the reaction now purple in color; neutral litmus paper turned blue). The reaction was extracted with chloroform (3 × 50 mL) and the organic phase was washed with water (3 × 30 mL) and brine (40 mL). The organic phase was dried over anhydrous Na₂SO₄, evaporated, and dried under vacuum for 0.5 h. The product was obtained in 48 % yield (0.174 g) as a dark purple solid with mp 159-163 °C. This material was sublimed under vacuum to give a colorless to very pale pink solid with mp 173-174 (d) °C. This material must be protected from light and used as soon as possible, to limit discoloration. Calculated for C₁₀H₆N₆: C 57.14%, H 2.88%, N 39.98%, found C 57.16%, H 2.73%, N 39.95%. IR (KBr, ν cm⁻¹): 2167, 2118 (N₃) (no amine present). ¹H NMR (300 MHz, CDCl₃): δ 7.30 (d, *J* = 7.35 Hz, 2H), 7.49 (t, *J* = 7.53 Hz, 2H), 7.90 (d, *J* = 8.2 Hz, 2H). ¹³C NMR (75.46 MHz, CDCl₃): δ 113.82, 118.23, 124.84, 126.27, 135.42.



Matrix-Isolation FTIR and UV-vis Spectroscopy. Matrix experiments were performed by means of standard techniques^{2,3} using an Iwatani Cryo Mini closed-cycle helium cryostat. For IR experiments, a CsI window was attached to the copper holder at the bottom of the cold head. Two opposing ports of a vacuum shroud surrounding the cold head were fit with KBr with a quartz plate for UV irradiation and a deposition plate for admitting the sample and matrix gas. For UV experiments, a sapphire cold window and quartz outer window were used. The temperature of the matrix was controlled by an Iwatani TCU-1 controller (gold vs chromel thermocouple). Irradiations were carried out with a Wacom 500-W xenon high-pressure arc lamp. For broad-band irradiation, Toshiba cutoff filters were used (50 % transmittance at the wavelength specified). Irradiations at >350 nm were carried out at intervals for up to 100 min, followed by short wavelength irradiations at 254 nm for an additional 240 min.

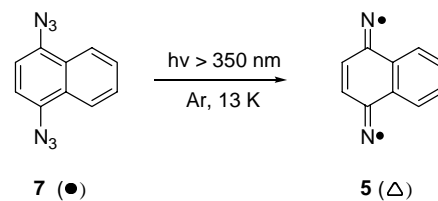
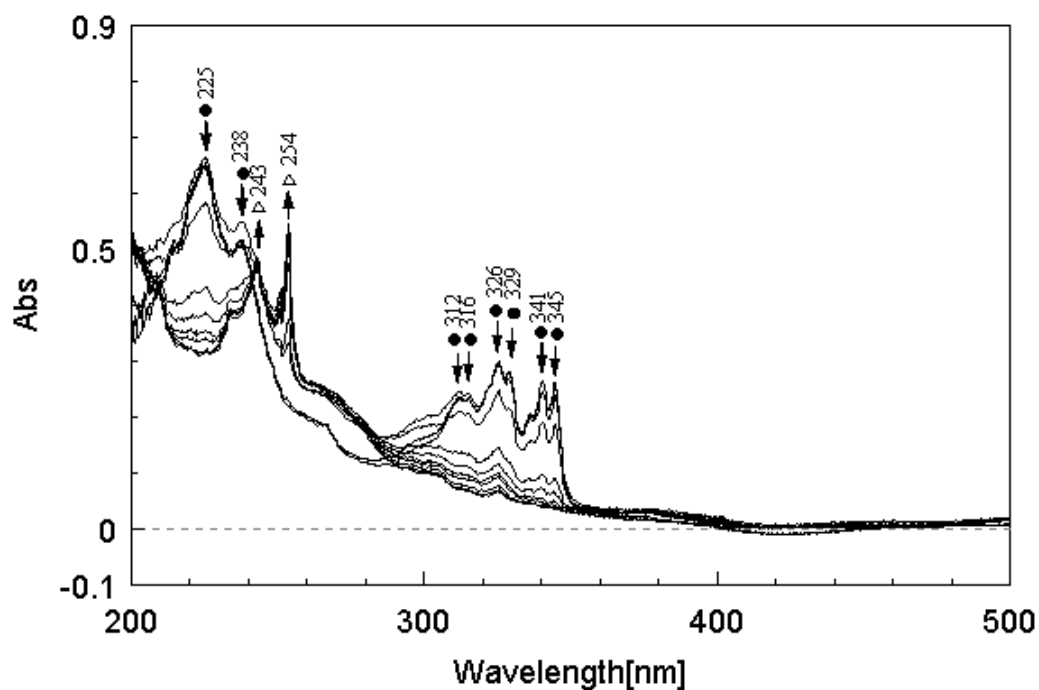
Frozen Matrix ESR Spectroscopy. Approximately 2 mg of **7** or **8** was dissolved in freshly distilled 2-methyltetrahydrofuran and placed in an ESR tube equipped with vacuum seals. The sample was subjected to several freeze-pump-thaw cycles before being finally frozen in liquid nitrogen and photolyzed. The photolysis for **7** was carried out through a Pyrex filter. The photolysis for **8** was carried out through an Oriel filter (#51830) for a total of 7 min. Other experiments were carried out for more extended times and with varying filters, including use of a monochromator at 350 nm. Upon thawing and refreezing all peaks assigned to reactive intermediates disappeared.

1) Hall, J. H.; Patterson, E. *J. Am. Chem. Soc.* **1967**, 89, 5856.

2) Tomioka, H.; Ichikawa, N.; Komatsu, K. *J. Am. Chem. Soc.* **1992**, 114, 6045.

3) McMahon, R. J.; Chapman, O. L.; Hayes, R. A.; Hess, T. C.; Krimmer, H. P. *J. Am. Chem. Soc.* **1985**, 107, 7597.

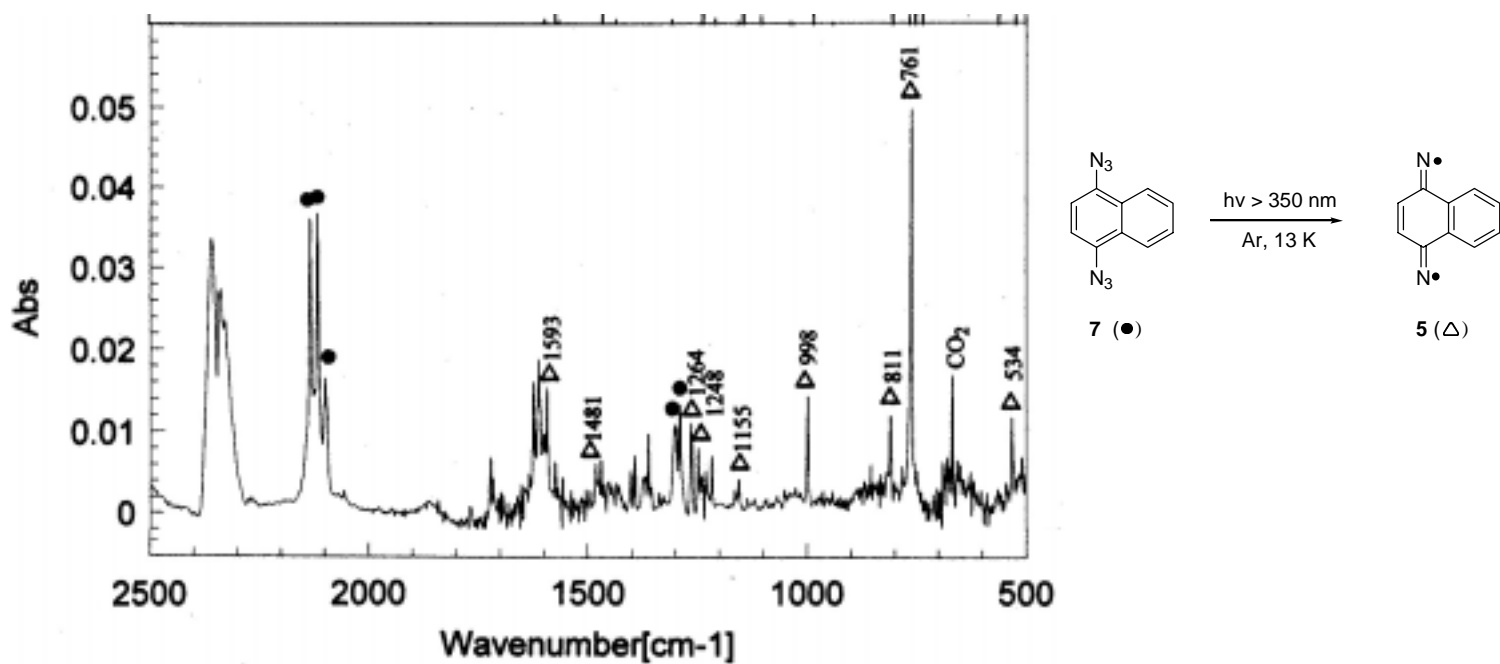
Matrix UV-vis Photolysis Experiment



Upper curve: Photolysis of **8** at >350 nm at intervals, 13 K, Ar matrix. Filled circles indicate bands from precursor **8**, open triangles indicate bands attributed to diiminediyl **5**.

Lower curve: Photolysis of **8** at >350 nm for 100 min, then at 254 for 240 min at intervals, 13 K, Ar matrix. Open circles indicate new bands attributed to ring opened product **9**, open triangles indicate bands attributed to diiminediyl **5**.

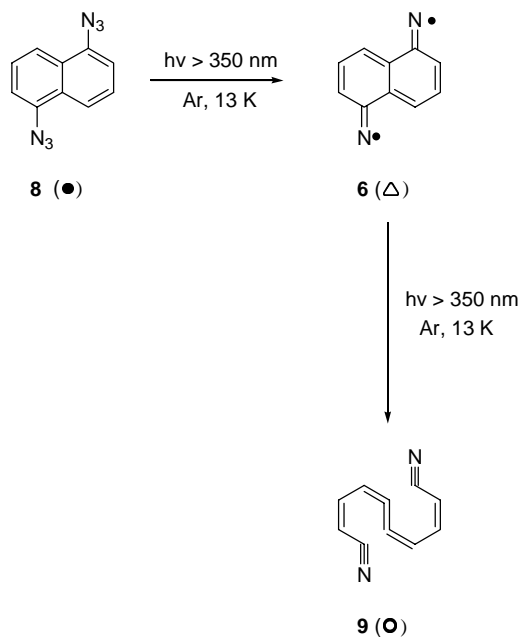
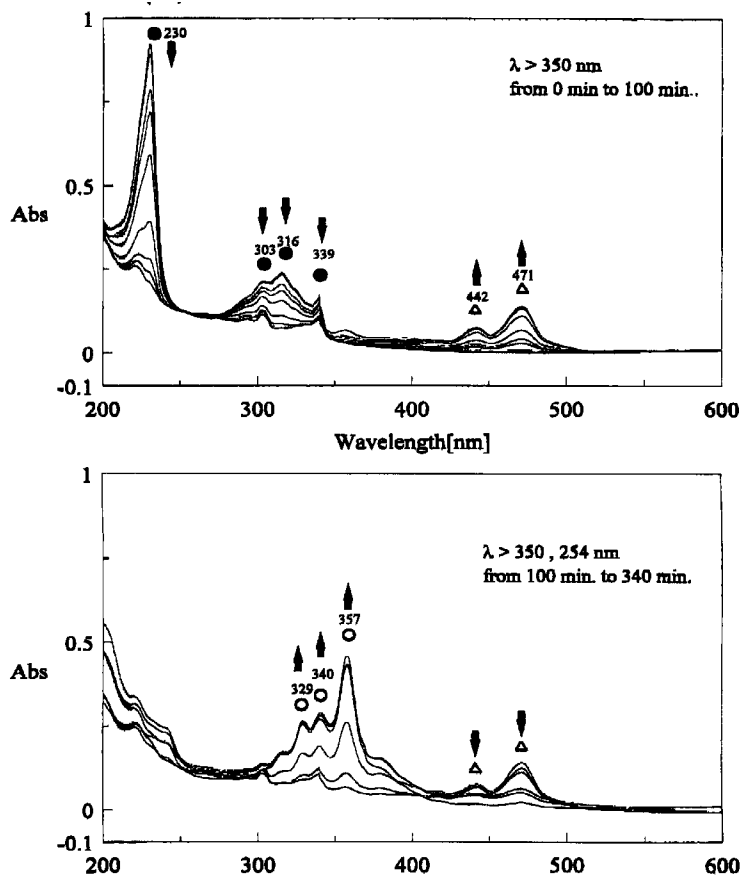
Matrix FTIR Photolysis Experiment



Upper curve: Photolysis of **8** at $>350 \text{ nm}$ at intervals, 13 K, Ar matrix. Filled circles indicate bands from precursor **8**, open triangles indicate post-photolysis bands attributed to diiminediyl **5**.

Lower curve: Photolysis of **8** at $>350 \text{ nm}$ for 20 min, then at 254 for 300 min at intervals, 13 K, Ar matrix. Open circles indicate new bands attributed to ring opened product **9**, open triangles indicate bands attributed to diiminediyl **5**.

Matrix UV-vis Photolysis Experiment



Upper curve: Photolysis of **8** at >350 nm at intervals, 13 K, Ar matrix. Filled circles indicate bands from precursor **8**, open triangles indicate bands attributed to diiminediyl **5**.

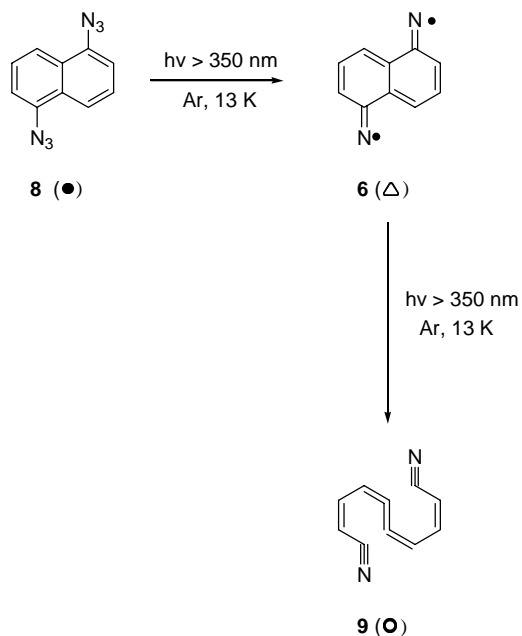
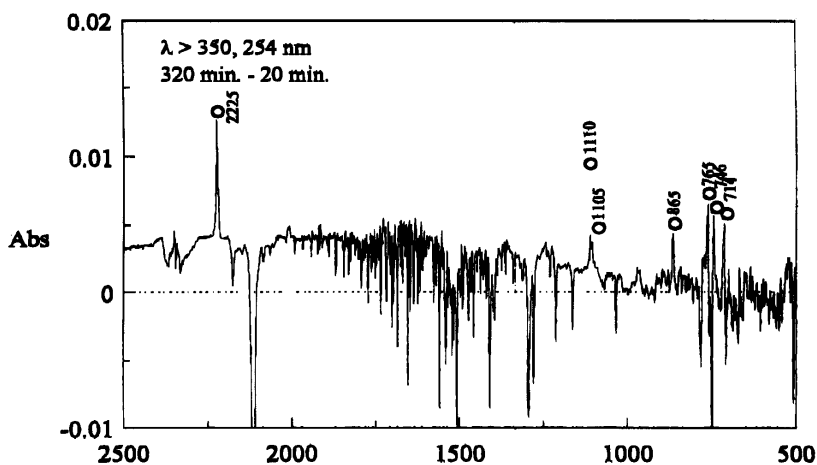
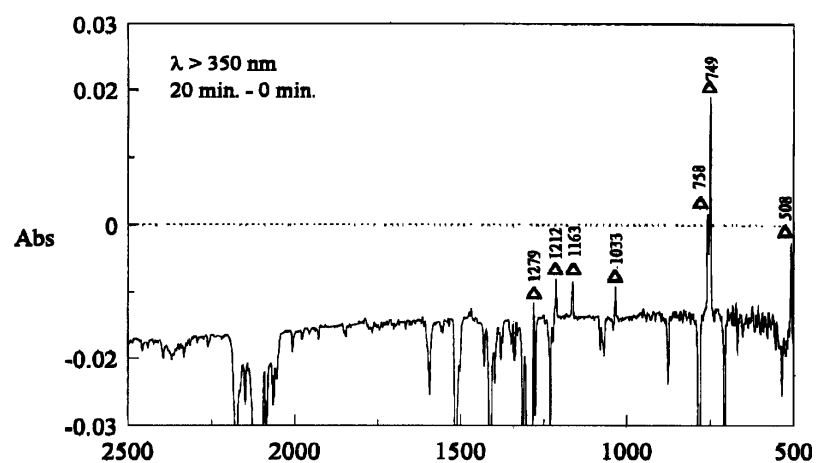
Lower curve: Photolysis of **8** at >350 nm for 100 min, then at 254 for 240 min at intervals, 13 K, Ar matrix. Open circles indicate new bands attributed to ring opened product **9**, open triangles indicate bands attributed to diiminediyl **5**.

Use of Hyperchem Pro 5.1 for Personal Computer (Hypercube Inc., 1997) using the ZINDO/S method with the UB3LYP/6-31G* biradical geometry, 10 occupied and 10 virtual orbitals, default parameterization in other aspects gives the following results. Bands predicted to have an oscillator strength of <0.001 in the 300-800 nm region are not listed.

	Assigned Experimental Wavelength (nm)	Computed Wavelength (nm)	Computed Oscillator Strength
Singlet ZINDO/S-CIS(10,10)		400	0.14
	442	455	0.25
	471	465	0.42
		566	0.07
Triplet ZINDO/S-CIS(10,10)		405	0.60

For further details about the ZINDO/S method with configuration interaction (CIS), see Zerner, M. C.; Ridley, J. E. *Theor. Chim. Acta* **1973**, 32, 111-134; *Ibid.* **1976**, 42, 223-236. For some further details about the use of the ZINDO/S methodology for open-shell molecules, see Seeger, D. E.; Lahti, P. M.; Rossi, A. R.; Berson, J. A. *J. Am. Chem. Soc.* **1986**, 108, 1251.

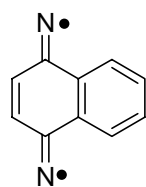
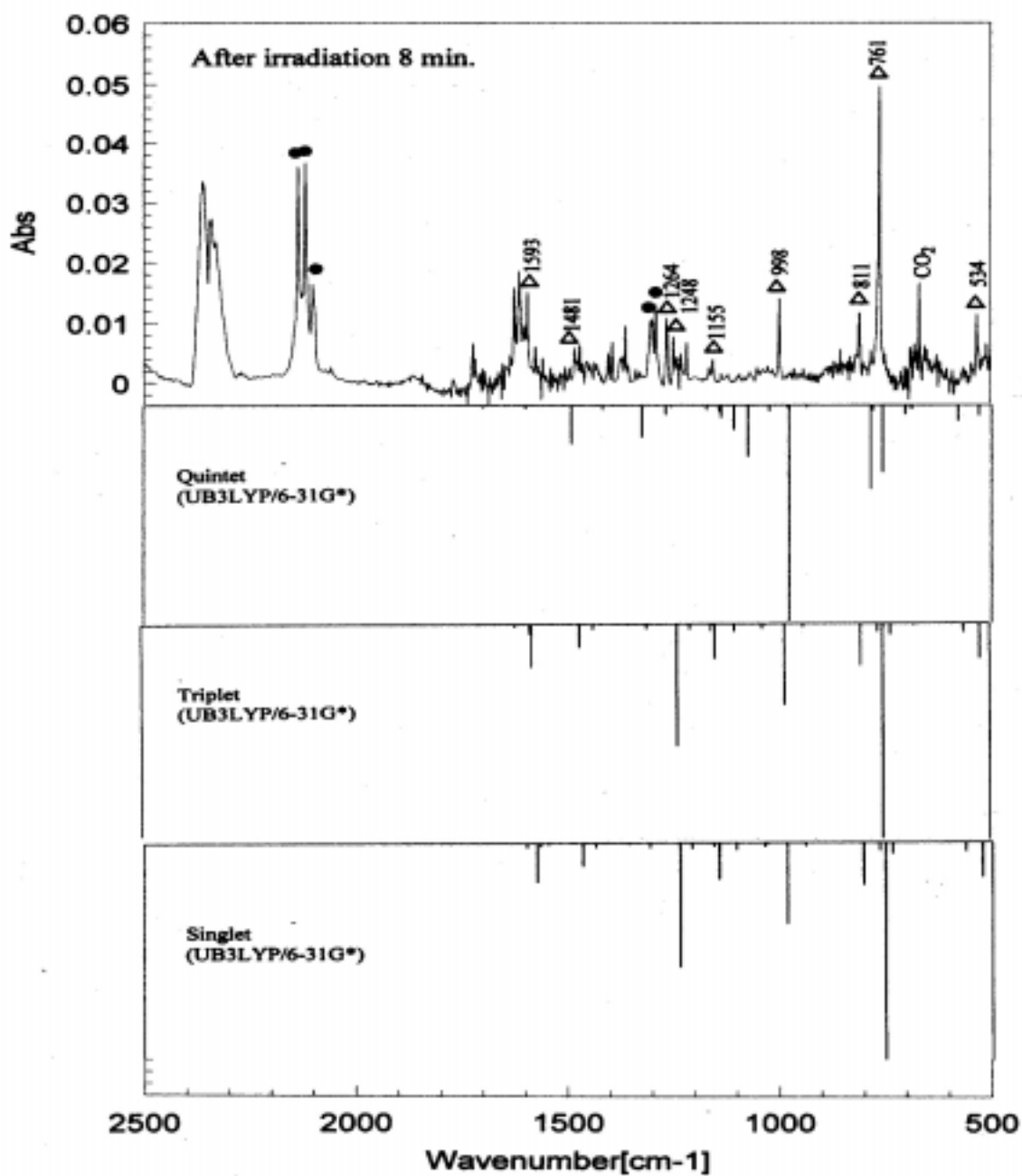
Matrix FTIR Photolysis Experiment



Upper curve: Photolysis of **8** at >350 nm at intervals, 13 K, Ar matrix. Filled circles indicate bands from precursor **8**, open triangles indicate bands attributed to diiminediyl **5**.

Lower curve: Photolysis of **8** at >350 nm for 20 min, then at 254 nm for 300 min at intervals, 13 K, Ar matrix. Open circles indicate new bands attributed to ring opened product **9**, open triangles indicate bands attributed to diiminediyl **5**.

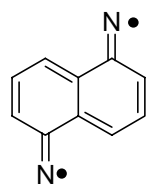
Comparison of UB3LYP/6-31G* Computed IR Bands to Experiment for 5

5 (Δ)

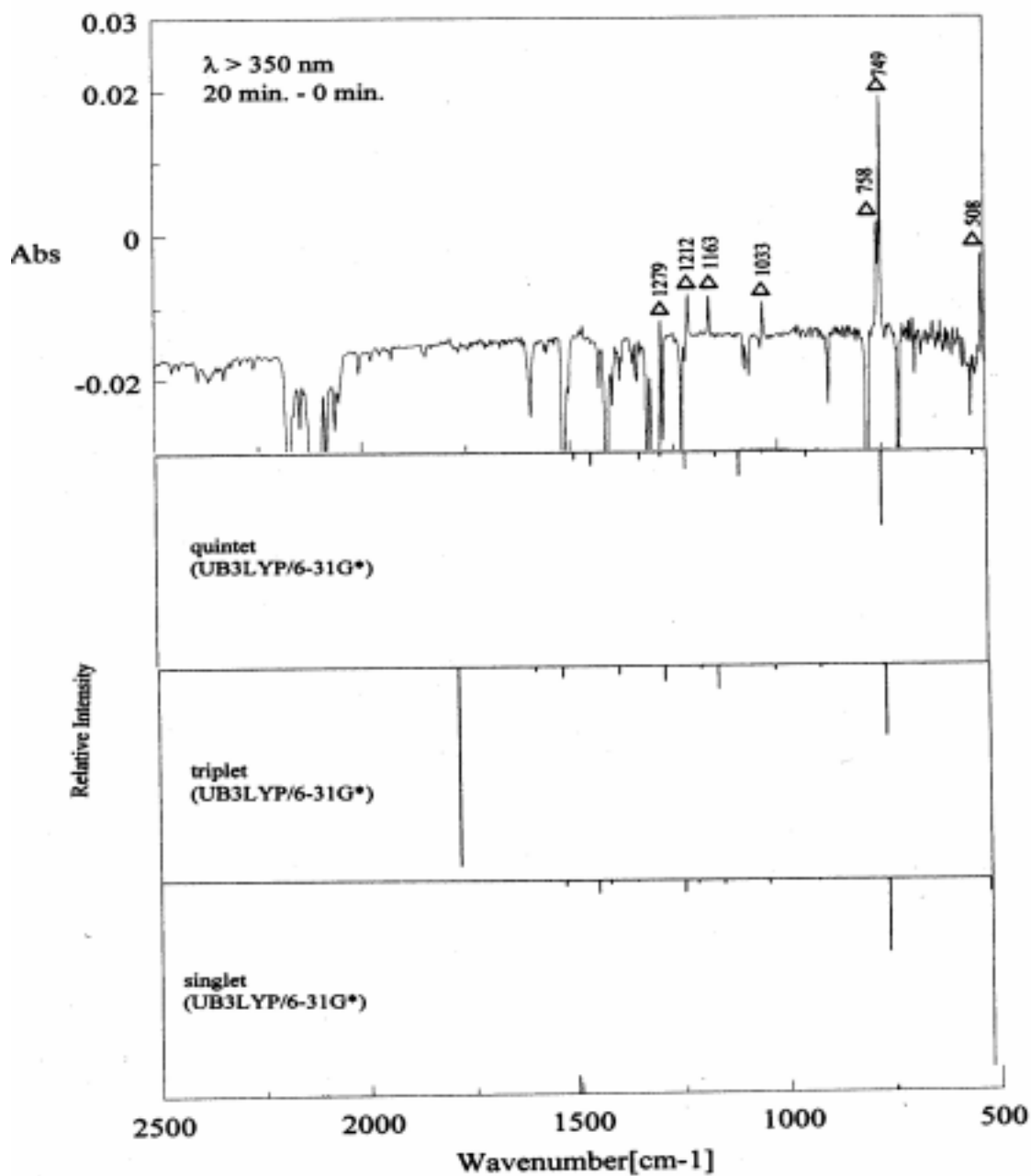
Top curve is experimental photolysis of 1,4-diazide **7** at 13 K, >350 nm. Bands marked with an open triangle grow in only after photolysis.

Lower three curves display UB3LYP/6-31G* computed vibrational band positions and intensities for singlet, triplet, and quintet states of 1,4-diiminediyl **5**. Singlet computation used a UB3LYP/GUESS=MIX wavefunction.

Comparison of UB3LYP/6-31G* Computed IR Bands to Experiment for **6**



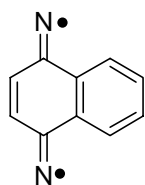
6 (Δ)



Top curve is experimental photolysis of 1,5-diazide **8** at 13 K, >350 nm. Bands marked with an open triangle grow in only after photolysis.

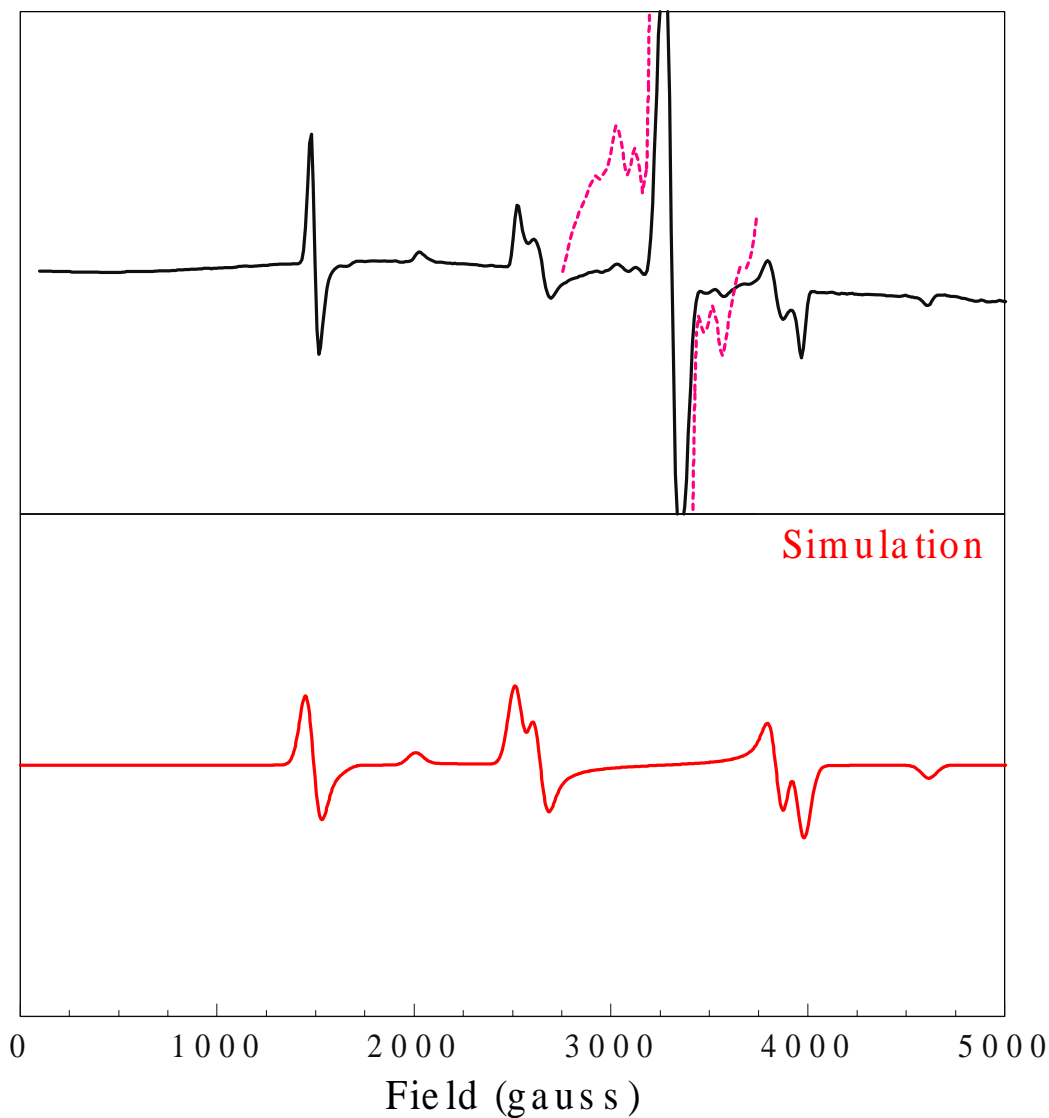
Lower three curves display UB3LYP/6-31G* computed vibrational band positions and intensities for singlet, triplet, and quintet states of 1,5-diaza-1,5-dihydro-1,5-diazide **6**. Singlet computation used a UB3LYP/GUESS=MIX wavefunction.

Comparison of Experimental and Simulated ESR Spectra for 5.



5

1,4-Naphthalenedinitrene (77 K, MTHF)



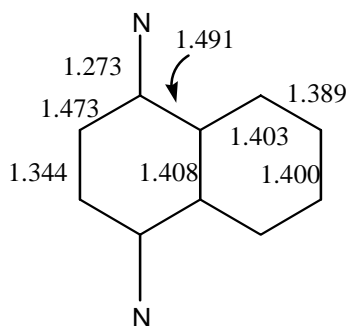
Top curve is experimental ESR spectrum obtained by photolysis of diazide **7** at >300 nm in MTHF, 77 K. The dotted purple trace is a 10-fold blowup of the 2750-3750 G region. The large peak at 3400 G is due to radical produced during the photolysis.

Lower curve shows spectrum simulated using the programs EFT and MKSPC (Sato, K. Ph. D. Thesis, Osaka City University, Osaka, Japan (1994)) with $\nu_0 = 9282$ MHz, $g(\text{isotropic}) = 2.0030$, $|D/hc| = 0.122$ cm $^{-1}$, $|E/hc| = 0.003$ cm $^{-1}$.

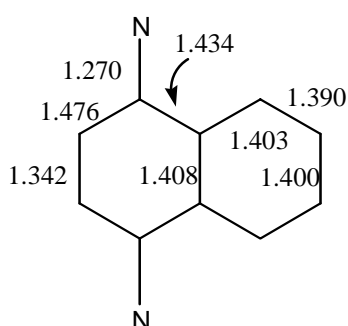
Computational Results for 5.

UB3LYP/6-31G* and CASSCF(6,6)/6-31G* optimized geometries and energies (singlet state computation carried out using GUESS=MIX keyword). Bond lengths in angstroms. Energies in hartrees. Spin squared expectation values taken directly from Gaussian 98 output for the UB3LYP computations.

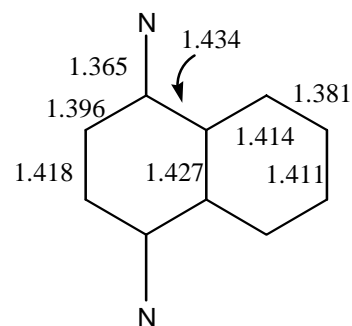
UB3LYP



5 (singlet)
-494.0559669
[<S²>=1.00]

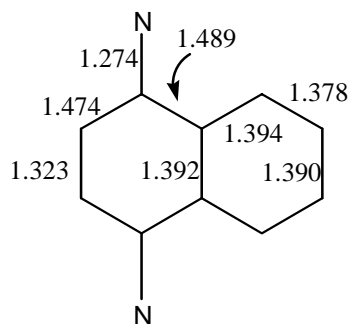


5 (³B₂)
-494.0549862
[<S²>=2.03]

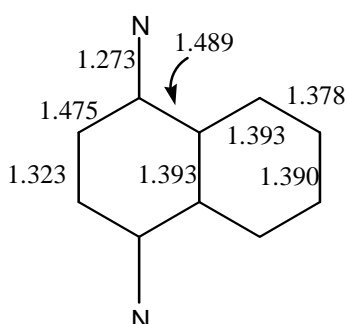


5 (⁵A₁)
-493.9929121
[<S²>=6.02]

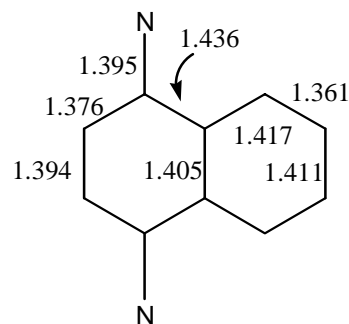
CASSCF(6,6)



5 (¹A₁)
-491.0618135



5 (³B₂)
-491.0613463



5 (⁵A₁)
-490.9844308

Comparison of Computational Results for 5.

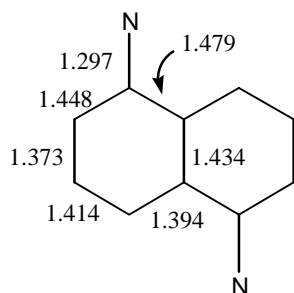
Table 1S. Total Energy of $^1\mathbf{5}$ ($E(^1\mathbf{5})$, hartree) and Relative Energies of $^3\mathbf{5}$ ($\Delta E(\text{S-T})$, kJ mol $^{-1}$) and $^5\mathbf{5}$ ($\Delta E(\text{S-Q})$, kJ mol $^{-1}$) with respect to $^1\mathbf{5}$.^a

	$E(^1\mathbf{6})$	$\Delta E(\text{S-T})$	$\Delta E(\text{S-Q})$
UB3LYP	-494.0559669	2.6	165.4
CASSCF(6,6) ^b	-491.0618135	1.2	203.0
CASSCF(14,14)//CASSCF(6,6) ^c	-491.1668367	2.7	(not done)
CASSCF(14,14)//CASSCF(12,12) ^d	-491.1679121	2.9	(not done)
CASPT2//CASSCF(6,6) ^{c,e}	-492.5851930	4.2	(not done)
CASPT2//CASSCF(12,12) ^{d,e}	-492.5866560	4.6	(not done)

- a. All computations use the 6-31G(d) basis set. Singlet is 1A_1 , triplet is 3B_2 , quintet is 5A_1 .
- b. Active space includes two π , two π^* MOs and the σ and σ^* MOs related with the "odd" electrons on the nitrogen centers.
- c. Computations done at CASSCF(6,6)/6-31G* geometries. Active space includes six π , six π^* MOs and the σ and σ^* MOs related with the "odd" electrons on the nitrogen centers.
- d. Computations done at CASSCF(12,12)/6-31G* geometries. Active space includes six π , six π^* MOs and the σ and σ^* MOs related with the "odd" electrons on the nitrogen centers.
- e. Using the CASSCF(14,14) wavefunction as reference. See note (d) for a description of the active space.

Computational Results for 6 versus 9.

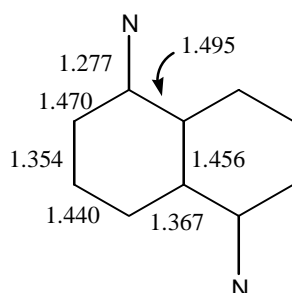
UB3LYP/6-31G* optimized geometries and energies (singlet state computations for both are carried out using GUESS=MIX keyword). Bond lengths in angstroms. Energies in hartrees. Spin squared expectation values taken directly from Gaussian 98 output.



6 (singlet)

-494.0257154

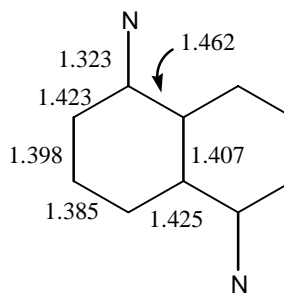
[$\langle S^2 \rangle$ = 1.78]



6 (3B_u)

-494.0179584

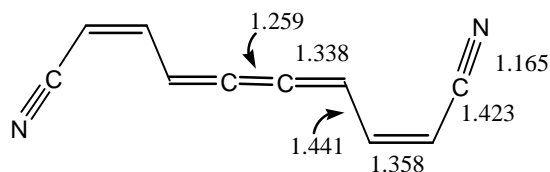
[$\langle S^2 \rangle$ = 2.03]



6 (5A_g)

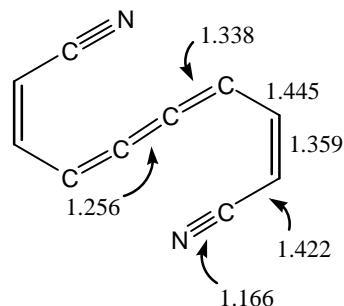
-494.0127401

[$\langle S^2 \rangle$ = 6.07]



9

-494.03471484



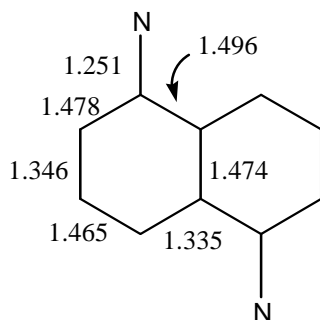
9

-494.0263425

Computational Results for **6**.

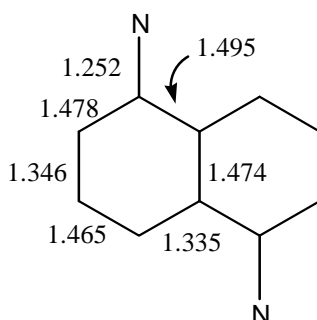
CASSCF optimized geometries and energies. Bond lengths in angstroms. Energies in hartrees.

CASSCF(6,6) / 6-31G*



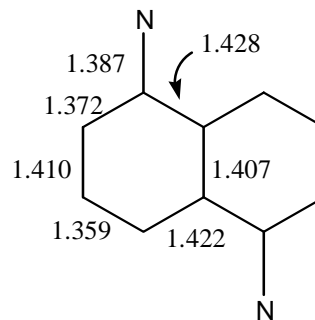
6 (1A_1)

-491.00292



6 (3B_u)

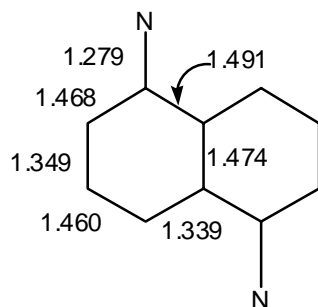
-491.00253



6 (5A_g)

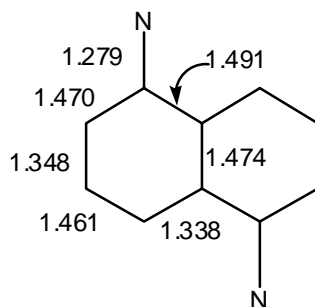
-490.98024

CASSCF(12,12)/6-31G*



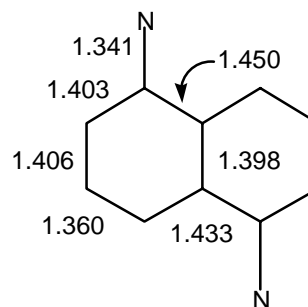
6 (1A_g)

-491.08071



6 (3B_u)

-491.07995



6 (5A_g)

-491.06002

Comparison of Computational Results for 6.

Table 2S. Total Energy of $^1\mathbf{6}$ ($E(^1\mathbf{6})$, hartree) and Relative Energies of $^3\mathbf{6}$ ($\Delta E(\text{S-T})$, kJ mol^{-1}) and $^5\mathbf{6}$ ($\Delta E(\text{S-Q})$, kJ mol^{-1}) with respect to $^1\mathbf{6}$.^a

	$E(^1\mathbf{6})$	$\Delta E(\text{S-T})$	$\Delta E(\text{S-T})$
UB3LYP	-494.02572	20.5	34.0
CASSCF(12,12) ^{b,f}	-491.08071	2.0	54.3
CASSCF(14,14) ^{c,d}	-491.13214	3.0	59.9
CASPT2 ^{d,e}	-492.54578	6.9	32.3
CASSCF(14,14) ^{c,f}	-491.13549	3.7	53.2
CASPT2 ^{e,f}	-492.55061	7.9	23.5

- f. All computations use the 6-31G(d) basis set. See Sanborn, J. A., Ph. D. Thesis, University of Massachusetts, Amherst, MA 01003, USA (2000) for 6-31G** results.
- b. Active space includes five π , five π^* MOs and the σ and σ^* MOs related with the "odd" electrons on the nitrogen centers. (Lowest occupied π and corresponding π^* not included in the active space).
- c. Active space includes six π , six π^* MOs and the σ and σ^* MOs related with the "odd" electrons on the nitrogen centers.
- d. CASSCF(2,2) optimized geometry for the singlet and ROHF/6-31G(d) optimized geometries for the triplet and quintet states.
- e. Using the CASSCF(14,14) wavefunction as reference.
- f. CASSCF(12,12) optimized geometries.